ChemPubSoc Europe

DOI: 10.1002/open.201900135

Open Access ChemistryOPEN Full Papers

Catalytic Chain Transfer Copolymerization of Propylene Oxide and CO_2 using Zinc Glutarate Catalyst

Jakob Marbach, Theresa Höfer, Nick Bornholdt, and Gerrit A. Luinstra*[a]

Oligo and poly(propylene ether carbonate)-polyols with molecular weights from 0.8 to over 50 kg/mol and with 60–92 mol% carbonate linkages were synthesized by chain transfer copolymerization of carbon dioxide (CO_2) and propylene oxide (PO) mediated by zinc glutarate. *Online*-monitoring of the polymerization revealed that the CTA controlled copolymerization has an induction time which is resulting from reversible catalyst deactivation by the CTA. Latter is neutralized after the first monomer additions. The outcome of the chain transfer reaction is a function of the carbonate content, *i.e.* CO_2 pressure, most likely on account of differences in mobility (diffusion) of the various polymers. Melt viscosities of poly(ether carbonate)diols with a carbonate content between 60 and 92 mol% are reported as function of the molecular weight, showing that the mobility is higher when the ether content is higher. The procedure of PO/CO_2 catalytic chain copolymerization allows tailoring the glass temperature and viscosity.

1. Introduction

The utilization of CO_2 as a feedstock in the chemical industry has got significant attention throughout the last decades as it is a potentially abundant, inexpensive and non-toxic raw material.[1,2] The alternating copolymerization of CO_2 with epoxides to form poly(alkylene carbonates) (PAC), *e.g.* poly (propylene carbonate) (PPC), is of particular interest as the copolymerization reaction is spontaneous and a number of epoxides can readily be made available on a larger scale. Some of the resulting materials exhibit properties such as biodegradability and biocompatibility,[3] have noticeable gas barrier properties, and can be relatively low in price.[4] A combination of these properties make these PACs predestined materials for short-term applications, *e.g.* for food packaging.[5,6] Applications for PACs with a higher added value are in form of sacrificial binding material,[6,7] as drug carrier[8–11] and as alternative (pseudo)soft component in polyurethane manufacturing.[12–18] Viable catalysts are required to commercialize PACs competitively as alternative plastic materials. Ever since Inoue's pioneering work, many studies have focused on the development of novel catalytic systems. Potent catalysts comprise metal complexes (Co, Cr, Zn) with macrocyclic porphyrin,[19–24] salen[25–38] or β-diiminate-type ligands[39–45] or heterogeneous compounds, such as ternary rare-earth metal/zinc-dialkyl mixtures,[46–49] double metal cyanide complexes (DMC)[50–58] and zinc dicarboxylates.[59–67]

Control over the molecular weight may be desirable, *e.g.* for use in water-based dispersions[68,69] or the application as polyol compound in polyurethane manufacturing.[70] Regulation of the molecular weight can be reached by the treatment of high-molecular weight products with acids or alcohols resulting in a controlled polymer degradation.[71,72] However, such procedures may be considered as industrially non-viable on account of the additional processing step. The requirement of extensive purification from low-molecular weight products and catalyst residues is further leading to additional costs. In contrast, immortal polymerization is a versatile method that allows the direct synthesis of end-functionalized polymers with tunable chain lengths and has the option of increasing catalyst productivity (TON).

The term immortal polymerization was initially introduced also by Inoue[73] for a living-type polymerization that involves a rapid, reversible chain transfer with protic chain transfer agents (CTA).[74] The chain transfer reaction occurs faster than the chain propagation step. The total number of chains formed thus exceeds the amount of initiator on a catalyst as dormant chain ends R—OH are reactivated by the proton exchange. Adjusting the monomer/CTA ratio allows to tailor the molecular weight of the final products.[73–75] On account of the rapid chain transfer, narrow molecular weight distributions are typically reached. The immortal polymerization has successfully been reported for the perfectly alternating copolymerization of propylene oxide (PO) and CO_2 catalyzed by homogeneous salen-complexes[76–78] and in the preparation of poly(ether carbonate) diols under the action of DMC catalysts.[79–86] The reporting on the molecular weight control using zinc dicarboxylates as copolymerization catalysts seems to be limited to an older patent.[87]

However, zinc dicarboxylates as used in this study have some attractiveness of mediating the PO/CO_2 copolymerization. They indeed have been used for decades in the first commercial preparation of PPC.[7] Catalytically active zinc carboxylates are

[a] J. Marbach, T. Höfer, N. Bornholdt, Prof. Dr. G. A. Luinstra
University of Hamburg
Institute of Technical and Macromolecular Chemistry
Bundesstraße 45, 20146 Hamburg
Germany
E-mail: luinstra@chemie.uni-hamburg.de

Supporting information for this article is available on the WWW under https://doi.org/10.1002/open.201900135

trivial to synthesize and to handle, are environmentally benign, have a reasonable activity and can have a high productivity.[64,88] Additionally and of more importance, the composition of the copolymer in terms of PO respectively of the CO_2 content can be tuned by temperature and pressure.[89] Potential products are thus ranging from poly(ether carbonates) to poly(carbonate ethers). This sets the herein described catalytic chain transfer copolymerization (CTCC) apart from procedures with the action of homogeneous complexes, *e.g.* of the Co(salen)-type. There, the product usually is a perfectly alternating copolymer of PO and CO_2, *i.e.* the carbonate contents of the main chain are $>$99 mol%. DMC catalysts on the other end of the "composition range" form predominantly poly(ether carbonates) with large contents of ether-blocks ($f_{carb} \ll 75$ mol%).[79] The zinc glutarate (ZnGA) mediated CTCC thus gives access to materials that cannot be obtained using current state-of-the-art Co(salen) or DMC catalysts.

Herein, the facile synthesis of OH-end-functionalized PO/CO_2 copolymers is reported with tunable chain lengths and tailored polymer composition using a nanoscopic ZnGA catalyst. The CCTC in the presence of various chain transfer agents has been studied in detail with respect to control over molecular weight and composition. The copolymerization process was monitored and insight into activity in dependence of CTA structure and concentration was gained.

The elementary reaction steps of the ZnGA are not known with certainty, but usually formulated with an anionic chain end binding to the catalyst surface. It is in that context generally accepted that PO is activated for ring opening by coordination to the catalyst surface. The reaction rate of copolymerization is most likely proportional to the amount of activated PO entities.[89] The coordination of PO stands in competition to that of CO_2 and also of CTAs. The ring opening leading to chain growth is effected by a nucleophilic chain end, in most reports by the alkoxide/carboxylate coordinated to the surface (Scheme 1). The propagating anionic chain ends in this mechanistic description can undergo an internal or additional protonation by the CTA, which is leading to a decoordination of R'OH/R'OC(O)OH. When this effective chain transfer is rapid relative to the insertion reactions, the result is a uniform propagation reaction. Alternatively, as formulated for DMC catalysis, also an hydroxyl entity of an external reagent ROH may directly attack the surface activated PO.[90] A proton transfer and decoordination of R'OH/R'OC(O)OH than is leading to the CCTC. Observations made in this study seem more compatible with an external nucleophilic attack of an OH entity, as proposed for the "catch up" kinetics of DMC catalyzed propoxylations. Carbonate entities arise when insertion of carbon dioxide into an intermediate metal alkoxide bond is competitive to decoordination. Ether linkages results from the consecutive addition of two or more PO units to the propagating chain end. The formation of cyclic propylene carbonate (cPC) may be observed to as the result of a backbiting reaction of a corresponding alcohol chain end.

Also, the rheological and thermal properties of the copolymers are reported upon. The material properties of the copolymers depend significantly on the polymer composition with respect to the ratio of carbonate to ether-linkages and their distribution. The polymer composition does not only affect the chain rigidity and thermal stability,[91] but also properties such as gas permeability[4,92] and is hence a key factor in the synthesis of tailored materials.

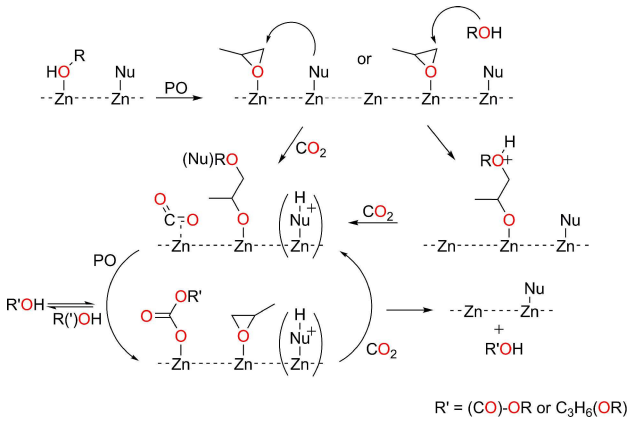

Scheme 1. Reaction pathways for the catalytic chain transfer copolymerization (CCTC) of CO_2 and PO with alcohols mediated by ZnGA.[77]

2. Results and Discussion

2.1. Chain Transfer Activity and Molecular Weight Control

The nanoscopic ZnGA catalyst system can be used to synthesize low-molecular weight oligo(propylene carbonate) in a catalytic chain transfer copolymerization (CCTC) with all the characteristics of an immortal copolymerization.[73,74] Initially, 2-phenoxyethanol was employed as a chain transfer agent (CTA). The presence of an aromatic entity in the otherwise aliphatic copolymer as the result of a successful chain transfer is easily detected in ^{1}H-NMR spectra. Analysis of the latter shows a low field shift of the signal of the *CH*$_2$-group adjacent to the phenoxy-end group and comparable changes in the signals of the aromatic system (Figure 1).

The incorporation of the CTA into the polymer is further indicated in the ESI-MS spectrum (Figure 2). The 2-phenoxyethoxy-terminated chains of $M_n \approx 900$ g/mol contain between

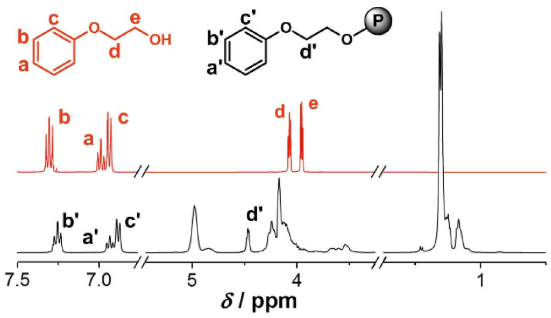

Figure 1. NMR spectra of low molecular weight PPC ($M_n \approx 900$ g/mol; black) and 2-phenoxyethanol (red). The protons of the second methylene group (e) are superimposed in the polymer spectrum.

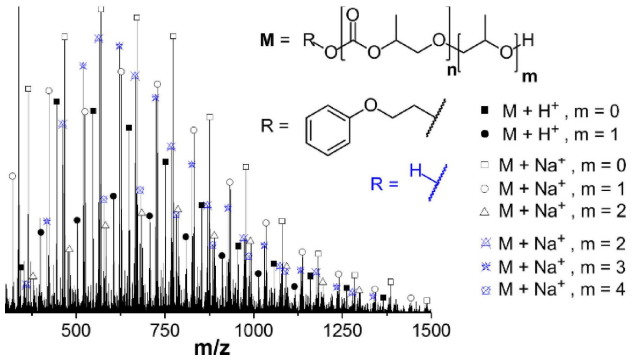

Figure 2. ESI mass spectrum of oligo(propylene carbonate) of $M_n \approx 900$ g/mol (Table 1, entry 6).

zero and two ether linkages per chain. Mass spectroscopy on higher molecular mass PPC is not readily achieved, and has rarely been reported upon.[93] Interestingly, chains carrying two OH-end groups were also detected, indicating that the copolymerization may also have been initiated by water, or less likely, an OH moiety tentatively originally present at the ZnGA-surface (vide infra). The existence of such functional groups on the catalytic surface of ZnGA has been proposed, but detection of these entities on the surface has remained difficult.[63,94,95]

The molecular weight of the oligo(propylene carbonate) product can be adjusted by varying the ratio between monomer and 2-phenoxyethanol as CTA (Table 1, Figure 3). The

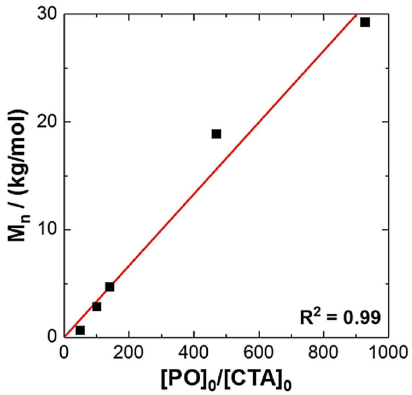

Figure 3. SEC-based M_n of the crude PPC vs. initial PO/CTA. 2-Phenoxyethanol is CTA.

molecular weight is relative to polystyrene standards: as the hydrodynamic volume of the poly(propylene carbonate ether)s is a function of the composition, a transformation using a universal approach seemed not more accurate.[96] The experimental results show that the molecular weights of the obtained polymers tend to correlate linearly with the PO/CTA ratio, *i.e.* the chain length can easily be tuned by varying the amount of CTA relative to PO. Thus, poly(ether carbonates) with number average molecular masses between 900 and 66.000 g/mol were obtained. The fact that the PDI does not significantly change upon addition of a CTA indicates that the chain exchange reaction occurs rapidly relative to the propagation reaction. Only at high CTA-concentrations a somewhat higher PDI is observed. The PDI values of the products are higher than one, contrasting to those of alternating PPC synthesized using discrete metal complexes[96] These are taken as the consequence of the heterogeneous composition of the product chains with respect to ether and carbonate content, and the backbiting reactions of intermediately formed chain ends. A broader distribution monomodal distribution with a PDI of 3–5 may thus be explained. The heterogeneous nature of ZnGA catalyst alone cannot have a major impact on the PDI as the chains would grow on several centers in CCTC.[77] Rather the presence of various end groups in form of 1- and 2-alkoxy and corresponding carboxylato entities leads to a distribution of propagation rates, broadening the Poisson distribution of an ideal living and regioselective alternating polymerization. PDIs larger than 6 are resulting from bimodal distributions, typically with small amounts of high molecular products (vide infra).

The polymer composition is not very dependent on the employed CTA concentration (Figure 4). The carbonate content is marginally lower at higher initial CTA concentrations. This may be related to the lower yields of copolymer under those conditions, which is accompanied by a higher fraction of cyclic propylene carbonate (cPC) f_{cPC} in the crude product. The backbiting reaction will proceed under such conditions with higher relative rates as a direct consequence of the increased concentration of free chain ends (Scheme 1).[97] Backbiting would proceed until an ether linkage is reached (ether linkages are formed by two consecutive PO insertions and constitute stable chain ends).[24] Consequently, the backbiting generally lowers the carbonate content in the remaining product.[97,98] The diols – chains formed from water (or OH– entities in the catalyst) consequently also tend to have a higher ether linkage

Table 1. CCTC using 2-phenoxyethanol as CTA.

Entry	PO/CTA [mol/mol]	TON[a] [–]	f_{carb}[b] [mol%]	f_{cPC}[b] [mol%]	$M_{n,NMR}$[c] [kg/mol]	$M_{n,SEC}$[d] [kg/mol]	$M_{w,SEC}$[d] [kg/mol]	PDI [–]
1	∞	988	91.7 ± 0.6	3.2 ± 0.5	-	66	296	4.5
2	930	1155	91.5	3.9	39	36	129	3.6
3	470	1073	91.5	4.5	25	26	87	3.4
4	140	1040	90.6	7.4	6.3	8.3	53	6.4
5	100	970	90.8	8.5	6.1	6.1	28	4.7
6	50	274	85.1	18.8	0.9	1.0	8.0	8.3

Reaction conditions: T = 60 °C, p = 30 bar, t = 4 h, V(PO) = 50 mL, m(ZnGA) = 100 mg. [a] in $[g_{PPC}/g_{Zn}]$, [b] determined from ^{1}H-NMR spectra, [c] absolute molecular weights were calculated by the equation $M_{n,\,NMR} = M_{RU}\,(A_{1.39\text{-}1.03}/3)\cdot(A_{6.90\text{-}6.85}/2)^{-1}$ with the average molecular weight of a repetition unit M_{RU}, [d] determined by SEC in THF against PS standards using RI detector mode.

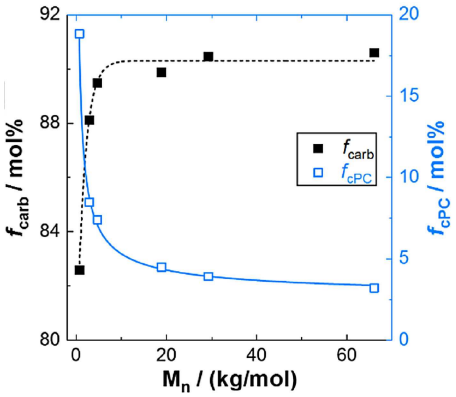

Figure 4. Content of carbonate linkages f_{carb} in the polymer and amount of cyclic by-product f_{cPC} as a function of the molecular weight, *i.e.* the concentration of end groups.

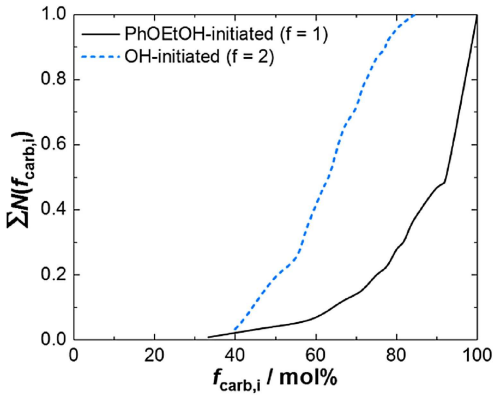

Figure 5. Cumulative distribution of the composition of monofunctional and bifunctional oligomers with $M_n \approx 900$ g/mol (Table 1, entry 6).

content than comparable mono-ols (Tables 1 and 2). The 2-phenoxyethoxy-initiated chains have only one chain end that can undergo a backbiting reaction to form cPC, whereas in case of water (or Zn–OH) initiated chains, the backbiting may proceed from both sides (Figure 5). The ether content of the diol- terminated chains accordingly is also higher ($f_{carb} = 63.4$ vs 88.5 mol%). The regioselectivity of the CCTC products remains unchanged to the copolymerization without a CTA (Figure S1) yielding oligo(ether carbonates) with about 66% head-to-tail-linkages.

The presence of 2-phenoxyethanol as CTA leads to a marginal higher yield of polymer at low CTA concentrations (Table 1). The catalysts average turnover frequency (TOF) increases by about 20% (~290 h^{-1}) relative to experiments without the use of a CTA (~250 h^{-1}). This may be related to a higher concentration of ring opening nucleophiles (at a minor loss of the amount of coordinated PO), and/or a better accessibility of the catalyst surface for smaller chains.[89] Higher concentrations of 2-phenoxyethanol, *i.e.* at PO/CTA ratios < 100, decrease the activity significantly. Latter is tentatively caused by an increasing CTA absorption on the ZnGA surface, which hampers PO monomer coordination. Similar observations were made before, *e.g.* for the higher concentration of CO_2 at higher pressures; the surface coverage with PO is determining the ZnGA performance.[89] The coordination of a CTA will reduce the concentration of activated PO-monomer, thus reducing the catalysts activity. These observations are reminiscent of the behavior of Zn–Co-DMC catalysts, which are also showing an induction time.[82,99,100] The induction period in these catalysts may be related to coordination of some entity on the surface; indeed CTAs of low molecular weight, like glycerin, may fully deactivate DMCs.[90]

Table 2. CCTC of PO/CO_2 with various CTAs.

Entry	CTA	PO/CTA [mol/moll]	TOF[a] [h^{-1}]	f_{carb}[b] [mol%]	f_{cPC}[b] [mol%]	$M_{n,NMR}$[c] [kg/mol]	$M_{n,SEC}$[d] [kg/mol]	$M_{w,SEC}$[d] [kg/mol]	PDI [–]
1	BPAF	250	124	92.3	3.3	11	11	60	5.3
2	BPS	1000	33	86.2	2.8	4.7	2.6	27	10.4
3	BPS	250	2	–	–	–	n.d.[g]	n.d.	n.d.
4	pBP	250	52	86.8	3.5	2.1	n.d.	n.d.	n.d.
5	MDBMP	250	182	88.9	5.2	6.5	5.0	39	7.8
6	HPBPA[e]	250	108	92.8	3.0	12	9.5	33	3.4
7	THTPM[f]	250	52	92.9	6.1	28	24	84	3.5
8	BPA	1000	274	92.0	3.3	56	37	144	3.9
9	BPA	500	241	91.5	2.8	23	23	107	4.6
10	BPA	250	167	91.6	2.4	9.4	8.9	55	6.1
11	BPA[h]	50	87	88.2	14.4	3.6[i]	3.9[i]	17[i]	4.4[i]
12	BPA[h]	25	38	78.6	12.9	0.8[i]	0.9[i]	7.3[i]	7.7[i]
13	HEBPA	1000	279	91.5	4.3	46	36	131	3.6
14	HEBPA	500	252	91.5	4.5	19	19	77	4.2
16	HEBPA	250	150	92.2	5.4	9.5	9.4	53	5.6

Reaction conditions: T = 60 °C, p = 30 bar, t = 4 h, V(PO) = 50 mL, m(ZnGA) = 100 mg, PO/CTA = 250. [a] in $[g_{PPC}/(g_{Zn} \cdot h)]$, [b] determined from ^{1}H-NMR spectra, [c] absolute molecular weights were calculated by the equation $M_{n,NMR} = M_{RU}\ (A_{1.39\text{-}1.03}/3) \cdot (A_{6.95\text{-}6.75}/x)^{-1}$ with the average molecular weight of a repetition unit M_{RU} and x = 4 (for MDBMP x = 2, for THTPM x = 6), [d] determined by SEC in THF against PS standards using RI detector mode, [e] primary/secondary OH ≈ 1/6 as determined by ^{1}H-NMR, [f] m(ZnGA) = 200 mg, t = 24 h, [g] not determined, [h] m(ZnGA) = 400 mg, t = 7 h, [i] determined from the crude reaction mixture.

2.2. Synthesis of PPEC-Diols

The CCTC was extended to bi- and trifunctional (in part commercially available) bisphenol-derived CTAs in order to synthesize tunable poly(propylene ether carbonate) PPEC-polyols (Scheme 2). The maiden CTAs contain both phenolic

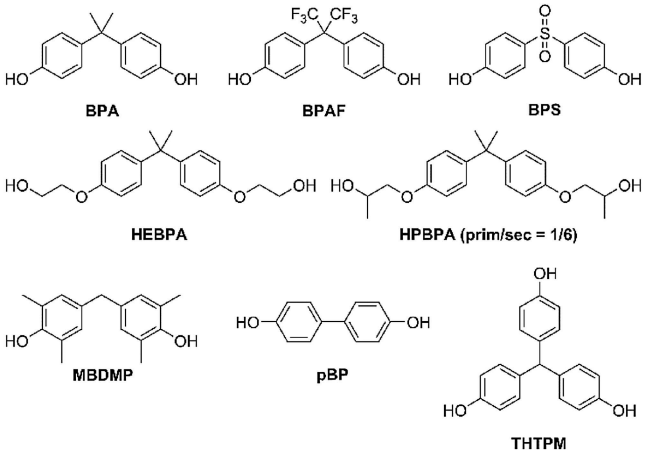

Scheme 2. Chain transfer agents.

and aliphatic hydroxyl moieties. Other aliphatic CTAs are also found effective (Tables S1 and S2). The use of CTAs with more than 2 OH-groups gives access to star-shaped polyols. Incorporation of these compounds into the polymeric product is also readily detected via NMR and SEC (UV/Vis detection mode). PPEC-polyols could thus be obtained for all derivatives except for higher concentrations of bisphenol S (BPS; Table 2). A severe retardation of the catalyst underlies the observation (vide infra). The catalysts selectivity (regarding carbonate vs ether linkages) remains unchanged, independent on the utilized CTA. Higher concentrations however decrease the catalysts productivity (Table 1). At the same time the formation of cPC is more pronounced as a consequence of the reduced molecular weights. For the low molecular weight products ($M_n < 50$ kg/mol) GPC-measured M_n is in reasonable agreement with the absolute values determined by NMR (Table 2).

2.3. *Online*-monitoring of the CCTC

Further insights into the CCTC were obtained by monitoring the copolymerization that was carried out as a batch reaction in PO while keeping the pressure CO_2 constant (semi-batch in CO_2). The concentration of PO was measured *online* using an IR-sensor (Figures 6 and 7), and the uptake of CO_2 was registered by means of a mass flow controller (Figure 8). Note that the concentration of PO during the copolymerization is dependent of its consumption and the associated dilution by the soluble copolymer. The corresponding uptake of CO_2 is modified by the release of CO_2 from the solution. PO is a much better solvent for CO_2 than the copolymer, and with conversion some CO_2 is

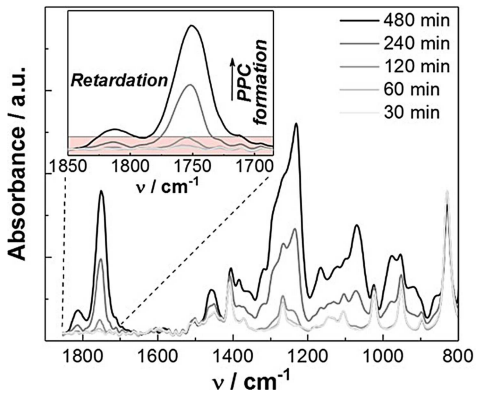

Figure 6. FT-IR spectra of the PO/CO_2 copolymerization using BPA as CTA (Table 3, entry 4).

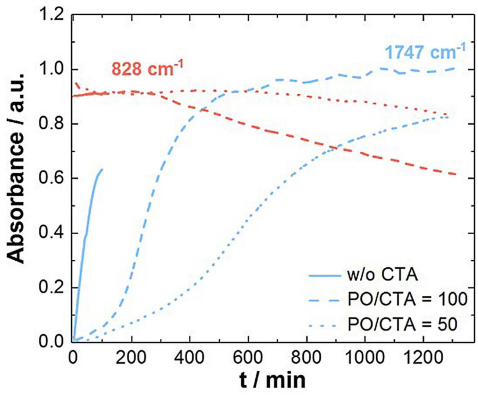

Figure 7. Absorbance of the C=O-stretching vibration of PPC (1747 cm^{-1}) and the ring vibration of PO (828 cm^{-1}) in time for various ratios of PO/BPA.

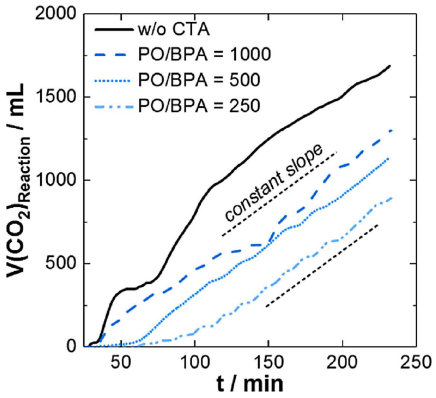

Figure 8. CO_2 uptake in dependence of the BPA concentration.

also liberated from the solution.[101] The evaluation of the data thus is elaborate. For that reason rate constants were not extracted although this is fundamentally possible.[102]

Data from both methods of reaction-monitoring indicate an initial period of little or no monomer conversion. The propagation rate increases substantially after this phase of inactivity. Larger amounts/concentrations of CTA prolong the initial period of retardation. In contrast, no retardation period is

observed for the PO/CO_2 copolymerization in the absence of a CTA (Figures 7 and 8).

BPA or HEBPA (ethoxylated BPA) as CTA show no significant differences in impact on the catalyst performance. The time-span necessary for activation of the catalyst is comparable at similar concentrations of BPA or HEBPA, and the resulting rate of copolymerization after the initial phase is the same within experimental variance (Tables 2 and S3). The formal ethoxylation of BPA to HEBPA, which is associated with the change from an aryloxy- to an alkoxy-type CTA, does not seem to fundamentally affect the chain regulation nor the catalysts performance (Figure 10). This is taken as evidence that the CTAs are preferentially consumed and that after consumption the catalyst inhibition by the CTA is released. The coordination of these CTAs to the ZnGA catalytic surface is apparently reversible. The combination of alkoxylation and carboxylation of the original CTAs yields compounds with a higher molecular mass. The coordination strength of the CTA decreases effectively in the process. The first propoxylation/carboxylation steps of the phenolic CTAs thus appear rate-limiting for the catalyst activity. BPA and HEBPA are preferentially consumed in the inhibition phase, *i.e.* are more reactive towards activated PO than the first alkoxylation products.

The induction time increases about exponentially with the concentration of BPA (Figures 8 and 9), illustrating the expected more than linear dependence of the rate of propoxylation on the concentration of BPA, blocking the surface and inhibiting its own conversion. The activity of the catalytic system after various amounts of BPA are consumed is the same within experimental error. A skew competition between reaction of the maiden CTAs and the products of the first PO/CO_2 additions of catalyst coordinated monomer leads to conversion of most of the CTAs and consequently to an increase in catalyst activity. The nature of the CTA and the primary products with respect to their nucleophilicity is a major factor in that.[103] The first PO/CO_2 addition(s) to the CTAs tend to majorly transform the primary alcohol or phenols into secondary hydroxyl entities, which are less readily reacting with activated PO (Scheme 3) and have a

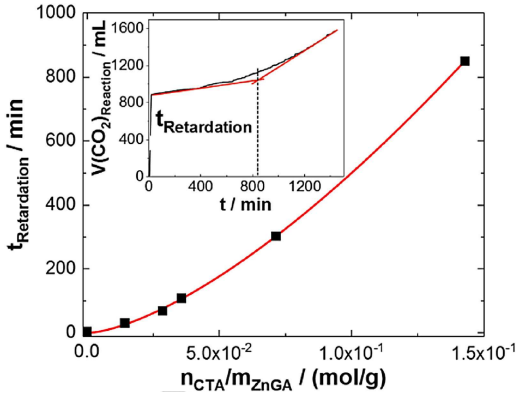

Figure 9. Length of the retardation period for various BPA/catalyst ratios. The retardation period is determined empirically from the intersection of the slope in early reaction stages after saturation with CO_2 and the constant slope after initial increase of the CO_2 consumption rate (inset). $V(CO_2)_{Reaction}$ refers to the uncorrected amount of CO_2 consumed.

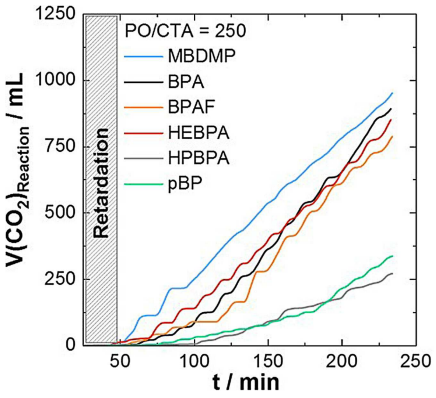

Figure 10. CO_2 consumption during the copolymerization with different CTAs.

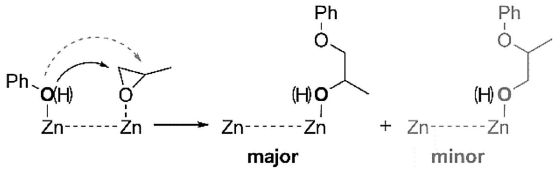

Scheme 3. Propoxylation of maiden CTA predominantly results in the formation of secondary alkoxylates.

lower OH number.[104,105] Same holds for BPAF and MDMBP that also give a similar rate of monomer conversion (Figure 10) after the induction period has passed in which the catalyst surface is blocked for PO coordination. In contrast, application of HPBPA – propoxylated BPA – as CTA results in overall reduced conversion rates in the same time span. The reached maximum copolymerization rate is much lower in the case of the propoxylated derivate after the same time of experiment with BPA or HEBPA. It obviously keeps on increasing over a much longer period and is thus slower to tentatively reach a similar maximum (Figure 10). Concomitantly, less of the CTA is incorporated into the copolymer, and the blocking of the catalyst surface partly sustains. This impact of HPBPA is as expected and consistent with the lower nucleophilicity of its predominantly secondary OH-groups relative to those of most of the primary alcohols and phenols in Scheme 2. The same appears to be the case for pBP and apparently in a more extreme form for BPS. A low initial concentration of BPS could only be tolerated for achieving an active catalyst system within a reasonable time. A lower rate of the starting reaction resulting from either a higher concentration of the CTA or less nucleophilic CTA also tends to broaden the distribution of the molecular weight (Table 2). The observations with regards to induction time/polymerization rate as function of time – in reversion – thus also would allow ranking the CTAs in coordination strength with respect to ZnGA.

2.4. Catalytic Action of ZnGA, Formation of High Molecular Weight Products

The initial high activity of the ZnGA catalyst typically decreases with conversion in several almost linear steps.[89] Similar is observed for the activity of the system under CCTC conditions after the induction time has passed. The monomer depletion does not appear to significantly influence the TOF at conversions lower than a critical value, like was found in previous studies of the nanoscopic ZnGA catalyst.[102] Deactivation of the catalyst was not of importance in that regard, and as it now turns out, molecular weight and concomitant inherent changes in the medium may influence the rate of copolymerization. It is found that the TOF in the first phase generally remains longer at the higher initial level, corresponding to a higher PO conversion upon addition of BPA. The first phase of the copolymerization is prolonged to a PO conversion in the range of ≈40%, which exceeds that of the unmodified copolymerization at ≈30% (Figure 11). The initial rates are comparable (Table 3).

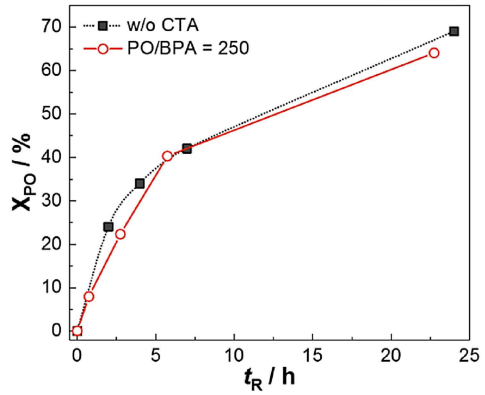

Figure 11. PO-conversion over time for the CCTC using BPA (red) and the copolymerization without the use of a CTA (black). t_R is the reduced reaction time, *i.e.* time of experiment without induction period.

When exceeding conversions of X_{PO}≈40%, the TOF decreases significantly, entering the second phase of almost linear rates.[89] The system of PO/CO_2/copolymer at X_{PO} > ~40% (molecular weight dependent) may be considered to become organogel-like, partly with a separated PO phase. The rate of propagation now also depends on the diffusion in the system and not so much on the catalyst itself. The polymer inhibits its own formation after exceeding the "critical conversion". The mobility of the chains and associated with that the mobility of chain ends decreases with the increasing polymer concentration and molecular weight. This also is more compatible with a copolymerization scheme with an external nucleophilic attack of an OH-moiety (Scheme 1). The occurrence of a limiting molecular weight is in that regard only to be expected, whereas in case of a catalyst based anionic chain end, a (slower) increase in molecular weight should occur. These mechanistic aspects will, however, need further attention in the future. Attempts to restore conditions of the initial phase by dilution with PO-monomer after 7 hours (≈40% PO conversion) were unsuccessful with regard of restoring the initial catalyst activity (Table 2, entry 9). The dilution or time to dissolve the gel apparently is not sufficient.

As mentioned above, smaller amounts of high molecular weight polymers may form during the CCTC reactions, leading to bimoda distributions. The high-molecular weight tails show up in the RI signal and are not readily detected by the UV-detector, illustrating the low concentration of the CTA chromophore in the product (Figure 12). This was in particular observed

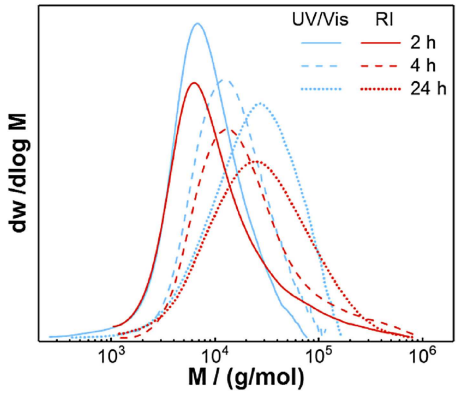

Figure 12. Molecular weight distributions of PPEC-polyols with 2-phenoxyethanol as CTA at various conversions (Table 1, entries 1, 2 and 4) using RI (solid) and UV/Vis (dashed) detector mode

in cases of higher CO_2 pressures (30 bars) leading to products with a carbonate content f_{carb} of ±90 mol% and is most likely to occur in the early phases (vide infra). The occurrence is chaotic as the (initial) products of lower molecular weight obtained at 30 bars randomly show PDIs between about 3 and 10 (Figure 13). This type of observations has also been made in DMC catalyzed alkoxylations using DMC catalysts.[90]

The high molecular weight tails are tentatively formed as a consequence of the initial irregular conditions in the reactor. It is a typical result of insufficient mixing, where chain growth resulting from monomer diffusion is faster than chain transfer, *i.e.* chain diffusion. The erratic formation possibly may be the

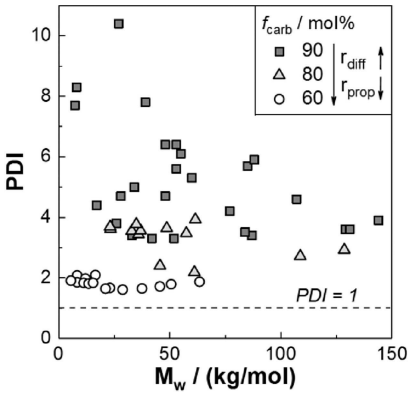

Figure 13. PDI of poly(propylene ether carbonate)-polyols of different compositions

Table 3. CCTC rate using BPA and HEBPA as CTA.

Entry	CTA	PO/CTA [mol/mol]	t [h]	TOF[a] [h^{-1}]	TON[b] [–]	X_{PO}[c] [%]	f_{carb}[d] [mol%]	$M_{n,NMR}$[d,e] [kg/mol]	$M_{n,SEC}$[f] [kg/mol]	$M_{w,SEC}$[f] [kg/mol]	PDI [–]
1	–	–	2	376	752	24	90.4	–	67	314	4.7
2	–	–	4	247	986	34	91.7	–	66	296	4.5
3	–	–	7	188	1315	42	90.9	–	91	327	3.6
4	–	–	24	84	2012	69	92.3	–	97	219	2.2
5	BPA	250	2	106	211	8	86.9	6.3	7.5	48	6.4
6	BPA	250	4	167	667	22	91.6	9.4	8.9	55	6.1
7	BPA	250	7	176	1232	40	91.3	15	15	85	5.7
8	BPA	250	24	81	1945	64	91.2	18	16	52	3.3
9[g]	BPA	250	24	82	1967	66	90.9	15	15	88	5.9
10	BPA	100	4	31	126	7	70.7	0.7	n.d.[h]	n.d.[h]	n.d.[h]
11	BPA	100	8	96	769	29	87.9	3.5	n.d.[h]	n.d.[h]	n.d.[h]
12	BPA	100	12	80	939	34	87.3	4.1	n.d.[h]	n.d.[h]	n.d.[h]
13	BPA	100	24	59	1407	49	87.9	5.8	n.d.[h]	n.d.[h]	n.d.[h]
14	BPA	100	48	37	1782	62	89.9	7.6	6.9	34	5.0
15	HEBPA	250	2	110	221	9	91.2	3.9	6.7	26	3.8
16	HEBPA	250	4	150	600	21	92.2	9.5	9.4	53	5.6
17	HEBPA	250	7	152	1062	35	91.3	11	10	48	4.7
18	HEBPA	250	24	69	1647	54	91.0	14	13	42	3.3

Reaction conditions T = 60 °C, p = 30 bar, V(PO) = 50 mL, m(ZnGA) = 100 mg, PO/CTA = 250. [a] in [$g_{PPC}/(g_{Zn} \cdot h)$], [b] in [g_{PPC}/g_{Zn}], [c] determined from the yield in/of the crude product, [d] determined from ^{1}H-NMR spectra, [e] absolute molecular weights were calculated using the equation $M_{n,NMR} = M_{RU}\,(A_{1.39\text{-}1.03}/3)\cdot(A_{6.95\text{-}6.75}/4)^{-1}$ with the average molecular weight of a repetition unit M_{RU}, [f] determined by SEC in THF and referenced against PS standards using RI detector, [g] Addition of 25 mL PO after 7 h, [h] could not be calculated due to superposition with cPC.

result of challenges of suspending the small amount of catalyst in PO. The high molecular product seems to be generated in a CTA independent reaction channel that becomes of importance at higher CO_2 pressures. It is alike the product generated in the ZnGA mediated copolymerization of PO and CO_2. These products reach a maximum molecular weight of $M_w \approx 200$ kg/mol, before growth is subsiding.[89] The direct copolymerization of PO and CO_2 has the highest rate at the 30 bars. This may the reason why bimodal product distributions are formed under such conditions, whereas CCTC is more competitive at lower pressures with a catalyst suspending in time. The initial higher PDIs of the products obtained at 30 bars of CO_2 pressure decrease with conversion (Figure 13). This is as explained above to be expected for a substantially living (/an immortal) copolymerization.

Consistently, products with a lower carbonate content do not show such a large variation in PDI and the high molecular weight tails are not formed (Figures 13 and 14). The PDIs of initial formed products are generally lower at lower pressures and are not so much dependent on conversion. Indeed, it is observed when performing the CCTC at 10 bar pressure of CO_2 (and T = 80 °C), leading to products with f_{carb} of 60 mol%, that the PDI is found at a constant level of about 1.8. Similar holds for experiments leading to products with a f_{carb} of 80 mol%, but with larger PDIs.

Note that the CCTC at 30 bars of CO_2 pressure still is the major process, and its dominance increases once the high molecular polymer reaches the "ceiling" molecular weight (Figure 15). Thus, using 2-phenoxyethanol as CTA, the maximum of the initial product distribution is shifted towards higher masses, whereas the high molecular tail remains more or less unchanged and is more and more overlapped by the CTA based product mass. This feature is more readily detected using higher concentrations of CTA *e.g.* in form of BPA, where the

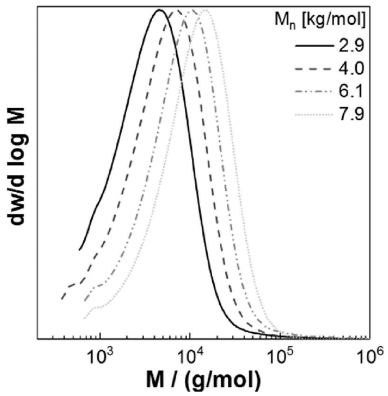

Figure 14. Molecular weight distributions for PPC-polyols with f_{carb} = 60 mol% (determined by SEC using RI detector mode).

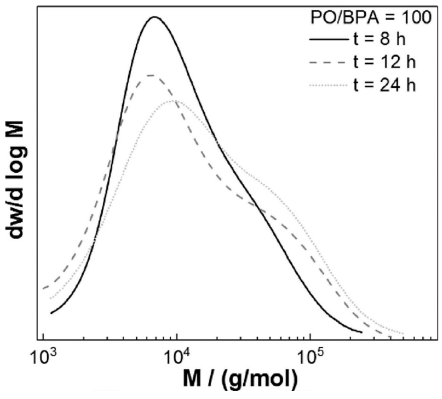

Figure 15. Time dependent molecular weight distributions for a PO/BPA CCTO at 30 bars of CO_2 pressure (f_{carb} = 90 mol%; RI detector).

main product remains lower in mass, and the formation of a bimodal distribution is indicated (Figure 15). The concentration of high molecular weight tail does not increase substantially, its mass increases to the value of about 200 kg/mol.

The molecular weights M_n of the obtained polymers correlate directly with the PO-conversion (X_{PO}), confirming the pseudo-living nature of the ZnGA catalyzed PO/CO_2 CCTC.[89] Catalysis at 30 bars of CO_2 pressure gives essentially uniform oligo(ether carbonates) independent of conversion with f_{carb} of ±90 mol% (Figure 16). This holds true even up to PO conversions above 50%.

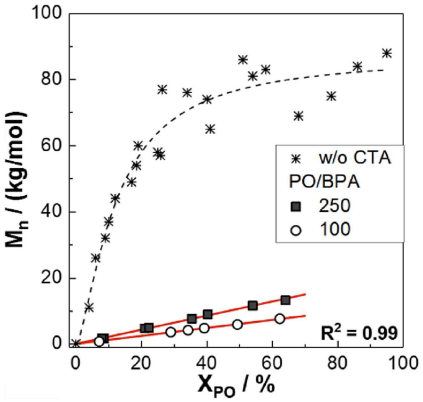

Figure 16. M_n (of the crude products) vs PO-conversion (X_{PO}) using BPA or HEBPA as CTA (Table 3, entries 5–18) in comparison with copolymerization without the use of a CTA (T = 60 °C, p = 30 bar; f_{carb} = 90 mol%).

2.5. Chain Mobility

The formation of more narrowly distributed products seems to result whenever the CCTC is dominant from the start. This is the case when the CO_2 pressure is lower than 30 bars and the rate of copolymerization is lower too. The formation of a second distribution seems to be the consequence of a lower exchange rate of larger growing chains (once formed) near the catalyst with chains in the bulk, *i.e.* relative to the propagation rate. These larger chains of lower mobility consequently grow at a higher rate as long the ceiling molecular weight is not reached, contrary to the concept of catch up kinetics observed for alkoxylation/ carboxy-lation of lower molecular weight CTAs. The balance between mobility and rate of polymerization would be determining the product distribution. Both are dependent on the reaction conditions, which thus determine the constitution of the product being formed. The rate of diffusion of the polymers resp. their viscosity is a function of the composition.[106] Chain mobility obviously is an important issue in the generation of poly(ether carbonate) diols, both with respect to conversion and chain regulation. It was thus decided to determine the melt viscosities of a series of products as function of molecular weight and composition. Melt viscosities can be taken as measure for the chain mobility: a melt resembles a theta solution of the polymer, which would be an acceptable model for the situation in the reaction medium of PO/CO_2 and in the organogel formed at higher conversions.

Poly(propylene ether carbonates) with various compositions are accessible by adjusting the reaction parameter *p* and *T* (Table S4).[89] It was found possible to prepare OH-terminated polycarbonates with controllable molecular weight and compositions between $f_{carb} \approx 60$ and 90 mol%. These products are typically closing the gap between poly(ether carbonates) obtainable by DMC catalysis[79] and the perfectly alternating poly(carbonates) obtained by *e.g.* Co-Salen catalysis,[107,108] *i.e.* when using a single catalyst.

Poly(propylene ether carbonates) with lower carbonate contents have substantial lower melt viscosities (Figure 17). The complex zero-shear viscosity $|\eta_0^*|$ of the polymer melts at 50 °C is approximately one order of magnitude lower for polymers with f_{carb} of 80 mol% than for those with f_{carb} of 90 mol%. The larger scattering of samples with f_{carb} of 90 mol% in the expected linear double logarithmic presentation of zero-shear viscosity versus weight average molecular mass is resulting from the individual distributions of the samples. These vary much more than those of f_{carb} of 60 or 80 mol% (Figure 13). The higher probability for random formation of a second distribution at higher CO_2 pressure is thus coincident with the relative lower mobility of the corresponding products. Consistently, the polymers with lower f_{carb} show more uniform and narrow molecular weight distributions even at high CTA-concentrations. It is therefore concluded that decreasing mobility of the chain segments can explain the occurrence of the second phase in the copolymerization and the formation of high molecular fraction at insufficient intermixing (Figures 12 and 15).

Controlling the viscosities of the products anyway is crucial with regards to processing the material, in particular in polyurethane manufacturing when mixing/demixing of chain extender, soft and hard phase components is proceeding. The molecular weight dependence of η_0 displays the importance of preventing the formation of high-molecular weight tails to maintain low product viscosities. The formation of such high-molecular weight side products is also been reported to occur during polyol-manufacturing when using DMC catalysts.[109]

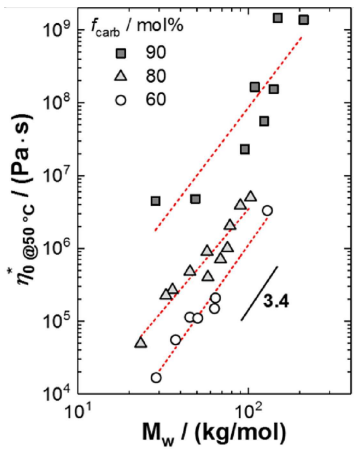

Figure 17. Zero-shear-viscosity η_0* at 50 °C for poly(propylene ether carbonates) of different carbonate contents and molecular weights.

The polymer composition is also determining the final material properties in extension to the molecular weight, which was found adjustable over the amount and type of CTA. This is of particular relevance to the glass temperature,[91] an important parameter when considering the poly(ether carbonate) polyols as polyurethane soft phase components. The glass transition temperature T_g as function of molecular weight and composition follows the Fox-Flory equation in first approximation (Figure 18).[110] T_g becomes more or less independent of the molecular weight M_n in between 15 and 25 kg/mol (Figure 19). Latter is an acceptable range for the broader distributed products, the entanglement molecular weight is expected in that range too.[91] Below the critical molecular weight of ~10 kg/mol, T_g drops rapidly.

3. Conclusions

Poly(propylene ether carbonate) polyols with tunable molecular weights and composition are accessible by means of the ZnGA-mediated immortal copolymerization of PO and CO_2. Aromatic BPA-derivates were found to be eligible CTAs. Control of the process parameters allows manipulating the composition of low-molecular weight PPC between f_{carb} = 60–92 mol%, thus, closing the compositional gap between poly(ether carbonates) and perfectly alternating PPC. The change in composition enables to tune the material properties, *e.g.* T_g and η of the final products in a certain range. The ZnGA-mediated immortal copolymerization of CO_2 and PO thereby gives access to products with a broader range of material properties. The formation of a high-molecular weight tail, in particular for polymers with high carbonate contents (f_{carb} ~90 mol%) seems to proceed independently from the CCTC. The broadening of the molecular weight distribution is explainable by the low mobility (exchange rates) of the growing chains relative to the propagation reaction. The catalytic action of ZnGA has thus all the characteristics of the DMC catalyzed alkoxylation and may hence proceed along the same mechanism.

Online-monitoring indicates an initial period of little or no monomer conversion that is related to slow first propoxylation steps of the CTAs. The concentration of the CTA should generally be held low to keep the induction period short. The addition of further CTA with a nucleophilicity over that of the average chain end during the CCTP could probably be tolerated once an initial conversion of PO has been reached. The molecular weights of the products can be easily tuned to values below 2000 g/mol by adjusting the PO/CTA ratio as well as the total monomer conversion. The addition of small quantities of CTA leads to an increase in the catalysts TOF of approx. 20% resulting in the highest activities for the zinc dicarboxylate-mediated copolymerization of CO_2 and PO reported to this date. The polymerization shows a pseudo-living behavior, *i.e.* M_n increases linear with the monomer conversion as no termination reactions occur to weight average molecular weight of about 200 kg/mol. The catalyst system has a higher activity as long as the gel has not formed, which is a function of conversion and molecular weight. The formation of such a gel in a living copolymerization is detrimental for control over the outcome. It puts a limitation to the conversion of PO, *i.e.* when performing the reaction in neat PO in batch.

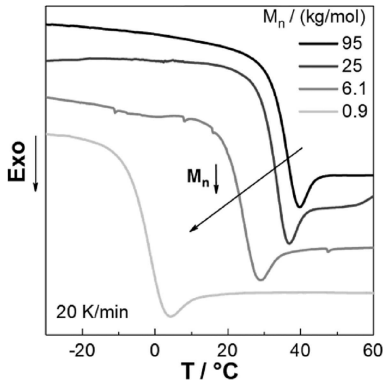

Figure 18. DSC curves for PPC of different molecular weights (f_{carb} = 90 mol%)

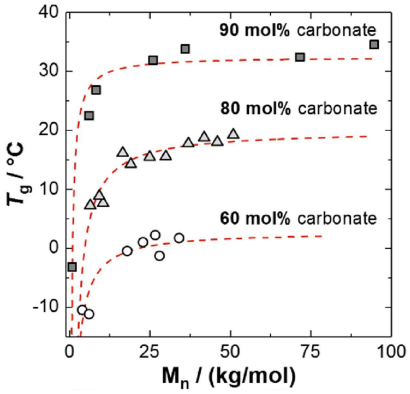

Figure 19. T_g of PPC with compositions of f_{carb} = 90–60 mol% as a function of molecular weight (right). The dashed lines represent a fit along the Fox-Flory equation $T_g = T_{g,\infty} - K/M_n$. The values for M_n are absolute determined by ^{1}H-NMR.

Experimental Section

Materials

Propylene oxide (PO) (99.9%, GHC Gerling, Holz & Co), CO_2 (99.995%, Linde Gas), 2,2-bis(4-hydroxyphenyl) propane (BPA, 97%, Sigma Aldrich), 4,4′-sulfonyl diphenol (BPS, 99%, Abcr Chemicals), 2,2-bis(4-hydroxyphenyl) hexafluoro propane (BPAF, 99%, Abcr Chemicals), 4,4′-dihydroxybiphenyl (97%, Sigma Aldrich), 4,4′-methylene bis(2,6-dimethylphenol) (MBDMP, 98%, Abcr Chemicals), sodium carbonate (>99.9%, Merck Millipore), ethylene carbonate (99%, Abcr Chemicals), propylene carbonate (>99%, Sigma Aldrich) were used as purchased. 2-Phenoxyethanol (PhOEtOH, 99%, Sigma Aldrich) was distilled and stored over molecular sieves (4 Å). ZnGA was synthesized as previously reported.[89] Alkoxylated BPA-derivates (HEBPA and HPBPA) and 4,4′,4″-Trihydroxyltriphenylmethane (THTPM) were synthesized according to the literature.[111–113]

Copolymerization of CO_2 and PO

Copolymerization experiments were carried out in 300 mL stainless steel autoclaves (Parr Instrument Company, Series 4560 Mini Reactors) equipped with 4-bladed propeller stirrers. The reactor was typically loaded with 100 mg of ZnGA and a specific amount of CTA, sealed and evacuated in order to remove all volatiles. After pressurizing with 10 bar of CO_2, PO was added (50 mL, 0.71 mol) with an HPLC pump (Bischoff Chromatography, HPD Multitherm 200). Subsequently, the reactor was heated to the desired temperature, and finally the pressure was adjusted to the target pressure. The pressure was kept constant with a feed of CO_2 gas, the uptake was monitored by means of a mass flow controller. Copolymerization was terminated by cooling the reactor to room temperature, releasing the pressure and degassing to remove residual PO. The resulting crude product was dissolved in acetone and precipitated in water or methanol repeatedly, in order to remove cyclic propylene carbonate (cPC). Polymer samples were dried *in vacuo* at 50 °C to a constant weight.

Experiments with *in situ*-FTIR-monitoring were performed in a 2 L stainless steel autoclave (Parr Instrument Company, Series 4520) equipped with an anchor agitator. The reactor was loaded with catalyst and the specific amount of CTA, evacuated and heated to the desired temperature. Subsequently, the reactor was pressurized with 30 bar of CO_2 and PO was added by means of an HPLC pump (Bischoff Chromatography, HPD Multitherm 200). The reaction progress was monitored using a ReactIR™ 45 FTIR equipped with a flexible probe having a diamond window. Spectra were recorded every 60 seconds at the range of $\nu = 650 - 2000\ cm^{-1}$.

Polymer Characterization

Product distribution and polymer composition were determined from ^1H NMR spectra. The spectra were recorded on a Bruker Avance Ultrashield-400 spectrometer in $CDCl_3$ at room temperature using tetramethylsilan as internal reference. The regioregularity of the polymers was determined from ^{13}C-IGATED-NMR spectra (2 000 scans). Molecular weight distributions were obtained using SEC (Flom Intelligent pump AI12, Schambek SFD RI2012 detector and HP 1050 series UV/Vis detector ($\lambda = 256$ nm), using a MZ-gel SDplus linear column (5 μm, 300×8 mm) in tetrahydrofuran as solvent. The values given are relative to monodisperse PS standards (Agilent). DSC measurements were conducted on a Mettler-Toledo DSC 1. The samples were subjected to a temperature cycles from −80 °C to 150 °C under a nitrogen atmosphere (heating rate of 10 K/min). The glass transition temperature was determined from the second heating cycle. Rheological experiments were performed on a DHR-2 combined motor-transducer rheometer (TA Instruments, New Castle, USA) using a plate-plate geometry (diameter = 8 mm, measuring gap = 1000 μm). Frequency sweeps were performed at T = 50–110 °C and angular frequencies of $\omega = 0.1$–100 rad/s. Experiments were performed within the linear viscoelastic regime, which was established in an amplitude sweep experiment. The dynamic viscosity as determined in shear experiments of the copolymers with molecular masses well-over entanglement molecular masses shows shear induced thinning. The frequency dependence of the viscosity was described using the Carreau-Yasuda equation $\eta(\omega) = \eta_\infty + (\eta_0 - \eta_\infty)[1 + (\lambda_0\omega)^b]^{n/b}$ with the infinite shear viscosity η_∞, the longest relaxation time λ_0 and the slope in the power law region n.[114] The fit parameter b accounts for the transition between Newtonian viscosity and the power law region. Specimen for rheometry measurements were prepared by solution casting from acetone solutions of the polymers. The resulting films were conditioned at 50 °C *in vacuo* prior to the measurements and were essentially free from cPC and solvents.

Conflict of Interest

The authors declare no conflict of interest.

Keywords: The authors would like to thank Dr. Felix Scheliga for bringing in his competence in the SEC measurements and their evaluation.

[1] T. Sakakura, J.-C. Choi, H. Yasuda, *Chem. Rev.* **2007**, *107*, 2365–2387.
[2] E. Alper, O. Yuksel Orhan, *Petroleum* **2017**, *3*, 109–126.
[3] G. Kim, M. Ree, H. Kim, I. J. Kim, J. R. Kim, J. I. Lee, *Macromol. Res.* **2008**, *16*, 473–480.
[4] F. Gao, Q. Zhou, Y. Dong, Y. Qin, X. Wang, Z. Xiaojiang, W. Fosong, *J. Polym. Res.* **2012**, *19*, 1–5.
[5] T. Dong, X. Yun, M. Li, W. Sun, Y. Duan, Y. Jin, *J. Appl. Polym. Sci.* **2015**, *132*, 41871.
[6] G. A. Luinstra, *Polym. Rev.* **2008**, *48*, 192–219.
[7] Empower Materials, www.empowermaterials.com (accessed December 2017).
[8] D. Peng, K. Huang, Y. Liu, S. Liu, H. Wu, H. Xiao, *Polym. Bull.* **2007**, *59*, 117–125.
[9] Y. Liu, D. Peng, K. Huang, S. Liu, Z. Liu, *J. Appl. Polym. Sci.* **2011**, *122*, 3248–3254.
[10] H. Li, Y. Niu, *Mater. Sci. Eng. C* **2018**, *89*, 160–165.
[11] H. Li, Y. Niu, *Int. J. Polym. Mater. Polym. Biomater.* **2018**, *67*, 192–198.
[12] J. Langanke, A. Wolf, J. Hofmann, K. Böhm, M. A. Subhani, T. E. Müller, W. Leitner, C. Gürtler, *Green Chem.* **2014**, *16*, 1865–1870.
[13] C. Xu, Z. Cai, J. Xing, Y. Ren, W. Xu, W. Shi, *Fibers Polym.* **2014**, *15*, 665–671.
[14] S. Liu, Y. Qin, X. Wang, F. Wang, *J. Renew. Mater.* **2015**, *3*, 101–112.
[15] J. Wang, H. Zhang, Y. Miao, L. Qiao, X. Wang, F. Wang, *Green Chem.* **2016**, *18*, 524–530.
[16] J. Wang, H. Zhang, Y. Miao, L. Qiao, X. Wang, F. Wang, *Polymer (Guildf).* **2016**, *100*, 219–226.
[17] P. Alagi, R. Ghorpade, Y. J. Choi, U. Patil, I. Kim, J. H. Baik, S. C. Hong, *ACS Sustainable Chem. Eng.* **2017**, *5*, 3871–3881.
[18] J. Wang, H. Zhang, Y. Miao, L. Qiao, X. Wang, F. Wang, *Polymer (Guildf).* **2018**, *138*, 211–217.
[19] H. Sugimoto, K. Kuroda, *Macromolecules* **2008**, *41*, 312–317.
[20] C. E. Anderson, S. I. Vagin, W. Xia, H. Jin, B. Rieger, *Macromolecules* **2012**, *45*, 6840–6849.
[21] C. E. Anderson, S. I. Vagin, M. Hammann, L. Zimmermann, B. Rieger, *ChemCatChem* **2013**, *5*, 3269–3280.
[22] C. Chatterjee, M. H. Chisholm, A. El-Khaldy, R. D. McIntosh, J. T. Miller, T. Wu, *Inorg. Chem.* **2013**, *52*, 4547–4553.
[23] X. Sheng, Y. Wang, Y. Qin, X. Wang, F. Wang, *RSC Adv.* **2014**, *4*, 54043–54050.
[24] X. Sheng, W. Wu, Y. Qin, X. Wang, F. Wang, *Polym. Chem.* **2015**, *6*, 4719–4724.
[25] D. J. Darensbourg, *Chem. Rev.* **2007**, *107*, 2388–2410.
[26] S. S, J. K. Min, J. E. Seong, S. J. Na, B. Y. Lee, *Angew. Chem. Int. Ed.* **2008**, *47*, 7306–7309; *Angew. Chem.* **2008**, *120*, 7416–7419.
[27] K. Nakano, S. Hashimoto, K. Nozaki, *Chem. Sci.* **2010**, *1*, 369.
[28] W.-M. Ren, Y. Liu, G.-P. Wu, J. Liu, X.-B. Lu, *J. Polym. Sci. Part A Polym. Chem.* **2011**, *49*, 4894–4901.
[29] B. Y. Lee, A. Cyriac, *Nat. Chem.* **2011**, *3*, 505–507.
[30] X.-B. Lu, D. J. Darensbourg, *Chem. Soc. Rev.* **2012**, *41*, 1462–1484.
[31] X.-B. Lu, W.-M. Ren, G.-P. Wu, *Acc. Chem. Res.* **2012**, *45*, 1721–1735.
[32] Y. Liu, W.-M. Ren, K.-K. He, X.-B. Lu, *Nat. Commun.* **2014**, *5*, 5687.
[33] M. Winkler, C. Romain, M. A. R. Meier, C. K. Williams, *Green Chem.* **2015**, *17*, 300–306.
[34] M. D. Konieczynska, X. Lin, H. Zhang, M. W. Grinstaff, *ACS Macro Lett.* **2015**, 533–537.
[35] Y. Liu, W.-M. Ren, W.-P. Zhang, R.-R. Zhao, X.-B. Lu, *Nat. Commun.* **2015**, *6*, 8594.
[36] S. Liu, X. Zhao, H. Guo, Y. Qin, X. Wang, F. Wang, *Macromol. Rapid Commun.* **2017**, 1600754.
[37] Y. Wang, D. J. Darensbourg, *Coord. Chem. Rev.* **2018**, *372*, 85–100.
[38] S. Klaus, M. W. Lehenmeier, C. E. Anderson, B. Rieger, *Coord. Chem. Rev.* **2011**, *255*, 1460–1479.

[39] J. G. Kim, C. D. Cowman, A. M. LaPointe, U. Wiesner, G. W. Coates, *Macromolecules* **2011**, *44*, 1110–1113.
[40] M. W. Lehenmeier, S. Kissling, P. T. Altenbuchner, C. Bruckmeier, P. Deglmann, A.-K. Brym, B. Rieger, *Angew. Chem. Int. Ed.* **2013**, *52*, 9821–6; *Angew. Chem.* **2013**, *125*, 10004–10009.
[41] W. C. Ellis, Y. Jung, M. Mulzer, R. Di Girolamo, E. B. Lobkovsky, G. W. Coates, *Chem. Sci.* **2014**, *5*, 4004.
[42] C. Li, R. J. Sablong, C. E. Koning, *Eur. Polym. J.* **2015**, *67*, 449–458.
[43] S. Kissling, M. W. Lehenmeier, P. T. Altenbuchner, A. Kronast, M. Reiter, P. Deglmann, U. B. Seemann, B. Rieger, *Chem. Commun.* **2015**, *51*, 4579–4582.
[44] M. Reiter, A. Kronast, S. Kissling, B. Rieger, *ACS Macro Lett.* **2016**, *5*, 419–423.
[45] M. Reiter, S. Vagin, A. Kronast, C. Jandl, B. Rieger, *Chem. Sci.* **2017**, *8*, 1876–1882.
[46] Y. Dong, X. Wang, X. Zhao, F. Wang, *J. Polym. Sci. Part A Polym. Chem.* **2012**, *50*, 362–370.
[47] Y. Tao, X. Wang, X. Chen, X. Zhao, F. Wang, *J. Polym. Sci. Part A Polym. Chem.* **2008**, *46*, 4451–4458.
[48] H. Lu, Y. Qin, X. Wang, X. Yang, S. Zhang, F. Wang, *J. Polym. Sci. Part A Polym. Chem. Chem.* **2011**, *49*, 3797–3804.
[49] L. Gu, Y. Qin, Y. Gao, X. Wang, F. Wang, *Chin. J. Chem.* **2012**, *30*, 2121–2125.
[50] X.-K. Sun, X.-H. Zhang, S. Chen, B.-Y. Du, Q. Wang, Z.-Q. Fan, G.-R. Qi, *Polymer (Guildf).* **2010**, *51*, 5719–5725.
[51] W. Zhang, L. Lu, Y. Cheng, N. Xu, L. Pan, Q. Lin, Y. Wang, *Green Chem.* **2011**, *13*, 2701–2703.
[52] Y. Dienes, W. Leitner, M. G. J. Müller, W. K. Offermans, T. Reier, A. Reinholdt, T. E. Weirich, T. E. Müller, *Green Chem.* **2012**, *14*, 1168–1177.
[53] T. E. Müller, C. Gürtler, M. Wohak, J. Hofmann, M. A. Subhani, M. Cosemans, W. Leitner, **2013**, EP 2548906.
[54] J. Sebastian, D. Srinivas, *Appl. Catal. A* **2014**, *482*, 300–308.
[55] Y. Zhang, X. Zhang, R. Wei, B. Du, Z. Fan, G. Qi, *RSC Adv.* **2014**, *4*, 36183–36188.
[56] X.-H. Zhang, R.-J. Wei, Y. Zhang, B.-Y. Du, Z.-Q. Fan, *Macromolecules* **2015**, *48*, 536–544.
[57] M. A. Subhani, B. Köhler, C. Gürtler, W. Leitner, T. E. Müller, *Angew. Chem. Int. Ed.* **2016**, *55*, 5591–5596; *Angew. Chem.* **2016**, *128*, 5681–5686.
[58] M. A. Subhani, C. Gürtler, W. Leitner, T. E. Müller, *Eur. J. Inorg. Chem.* **2016**, *2016*, 1944–1949.
[59] A. M. Sakharov, V. V. Il'in, V. V. Rusak, Z. N. Nysenko, S. A. Klimov, *Russ. Chem. Bull.* **2002**, *51*, 1451–1454.
[60] J. T. Wang, Q. Zhu, X. L. Lu, Y. Z. Meng, *Eur. Polym. J.* **2005**, *41*, 1108–1114.
[61] J.-S. Kim, H. Kim, J. Yoon, K. Heo, M. Ree, *J. Polym. Sci. Part A Polym. Chem.* **2005**, *43*, 4079–4088.
[62] M. Ree, Y. Hwang, J.-S. Kim, H. Kim, G. Kim, H. Kim, *Catal. Today* **2006**, *115*, 134–145.
[63] S. Klaus, M. W. Lehenmeier, E. Herdtweck, P. Deglmann, A. K. Ott, B. Rieger, *J. Am. Chem. Soc.* **2011**, *133*, 13151–13161.
[64] A. Brym, J. Zubiller, G. A. Luinstra, R. Korashvili, **2013**, WO 2013/034489.
[65] R. Korashvili, B. Nörnberg, N. Bornholdt, E. Borchardt, G. A. Luinstra, *Chemie Ing. Tech.* **2013**, *85*, 437–446.
[66] P. Sudakar, D. Sivanesan, S. Yoon, *Macromol. Rapid Commun.* **2016**, *37*, 788–793.
[67] P. Song, H. Xu, X. Mao, X. Liu, L. Wang, *Polym. Adv. Technol.* **2017**, *28*, 736–741.
[68] L. Ma, L. Song, F. Li, H. Wang, B. Liu, *Colloid Polym. Sci.* **2017**, *295*, 2299–2307.
[69] M. Scharfenberg, S. Wald, F. R. Wurm, H. Frey, *Polymer* **2017**, *9*, 422.
[70] Saudi Aramco, Press release, www.saudiaramco.com/en/news-media/news/2016/acquires-novomers-polyol-business-downstream-expansion (accessed March 2019).
[71] J. Courtois, M. Schneele, W. Riegel, A. K. Brym, H.-H. Görtz, **2012**, EP 2 557 104.
[72] W. Luo, J. Qin, M. Xiao, D. Han, S. Wang, Y. Meng, *ACS Omega* **2017**, *2*, 3205–3213.
[73] S. Asano, T. Aida, S. Inoue, *J. Chem. Soc., Chem. Commun.* **1985**, 1148–1149.
[74] S. Inoue, *J. Polym. Sci. Part A Polym. Chem.* **2000**, *38*, 2861–2871.
[75] K. Soga, K. Hyakkoku, S. Ikeda, *Die Makromol. Chemie* **1978**, *179*, 2837–2843.
[76] S. D. Allen, G. W. Coates, A. E. Cherian, C. A. Simoneau, A. Gridnev, J. J. Farmer, **2010**, WO 2010/028362.
[77] A. Cyriac, S. H. Lee, J. K. Varghese, E. S. Park, J. H. Park, B. Y. Lee, *Macromolecules* **2010**, *43*, 7398–7401.
[78] S. H. Lee, A. Cyriac, J. Y. Jeon, B. Y. Lee, *Polym. Chem.* **2012**, *3*, 1215.
[79] Y. Gao, L. Gu, Y. Qin, X. Wang, F. Wang, *J. Polym. Sci. Part A Polym. Chem.* **2012**, *50*, 5177–5184.
[80] Y. Gao, Y. Qin, X. Zhao, F. Wang, X. Wang, *J. Polym. Res.* **2012**, *19*, 9878.
[81] J. K. Varghese, D. S. Park, J. Y. Jeon, B. Y. Lee, *J. Polym. Sci. Part A Polym. Chem.* **2013**, *51*, 4811–4818.
[82] S. Liu, Y. Qin, X. Chen, X. Wang, F. Wang, *Polym. Chem.* **2014**, *5*, 6171–6179.
[83] S. Liu, Y. Miao, L. Qiao, Y. Qin, X. Wang, X. Chen, F. Wang, *Polym. Chem.* **2015**, *6*, 7580–7585.
[84] K. Ma, Q. Bai, L. Zhang, B. Liu, *RSC Adv.* **2016**, *6*, 48405–48410.
[85] S. Liu, Y. Qin, H. Guo, X. Wang, F. Wang, *Sci. China Chem.* **2016**, *59*, 1369–1375.
[86] S. Liu, Y. Qin, L. Qiao, Y. Miao, X. Wang, F. Wang, *Polym. Chem.* **2016**, *7*, 146–152.
[87] A. Rokicki, **1990**, US 4943677.
[88] S. Padmanaban, M. Kim, S. Yoon, *J. Ind. Eng. Chem.* **2019**, *71*, 336–344.
[89] J. Marbach, B. Nörnberg, A. F. Rahlf, G. A. Luinstra, *Catal. Sci. Technol.* **2017**, *7*, 2897–2905.
[90] M. Ionescu, *Chemistry and Technology of Polyols for Polyurethane*, **2008**.
[91] G. A. Luinstra, E. Borchardt, *Adv. Polym. Sci* **2012**, *245*, 29–48.
[92] X. Yun, X. Zhang, Y. Jin, J. Yang, G. Zhang, T. Dong, *J. Macromol. Sci. Part B* **2015**, *54*, 275–285.
[93] D. Hölting, Ph D thesis, *Kohlenstoffdioxid sowie 2,3-Butylenoxid-Derivate als Polymerbausteine -Synthese und Charakterisierung von Polyolen und ungesättigten Polyestern als Komponenten für Polyurethane und UP-Harze*, University of Hamburg, **2012**.
[94] M. H. Chisholm, D. Navarro-Llobet, Z. Zhou, *Macromolecules* **2002**, *35*, 6494–6504.
[95] J. Kim, M. Ree, S. Lee, W. Oh, S. Baek, B. Lee, T. Shin, K. Kim, B. Kim, J. Lüning, *J. Catal.* **2003**, *218*, 386–395.
[96] E. Borchardt, Ph D thesis, *Zur Rheologie Und Lichtstreuung von Poly (Propylencarbonat)*, University of Hamburg, **2014**.
[97] D. J. Darensbourg, S.-H. Wei, *Macromolecules* **2012**, *45*, 5916–5922.
[98] D. J. Darensbourg, A. D. Yeung, *Polym. Chem.* **2015**, *6*, 1103–1117.
[99] L. Wu, A. Yu, M. Zhang, B. Liu, L. Chen, *J. Appl. Polym. Sci.* **2004**, *92*, 1302–1309.
[100] S. H. Lee, I. K. Lee, J. Y. Ha, J. K. Jo, I. Park, C.-S. Ha, H. Suh, I. Kim, *Ind. Eng. Chem. Res.* **2010**, *49*, 4107–4116.
[101] J. M. S. Fonseca, R. Dohrn, A. Wolf, R. Bachmann, *Fluid Phase Equilib.* **2012**, *318*, 83–88.
[102] B. Nörnberg, C. Spottog, A. Rahlf, R. Korashvili, C. Berlin, G. A. Luinstra, *Macromol. Symp.* **2013**, *333*, 190–196.
[103] T. W. Coffindaffer, I. P. Rothwell, J. C. Huffman, *Inorg. Chem.* **1983**, *22*, 2906–2910.
[104] J. Reese, K. McDaniel, R. Lenahan, R. Gastinger, M. Morrison, Proceedings, 13th Annual Green Chemistry & Engineering Conference, IMPACTTM Technol. A Greener Polyether Process, acs.confex.com/acs/green09/recordingredirect.cgi/id/489.
[105] J. Pazos, E. Browne, in *Equiv. Weight Polym. Alkylene Oxides by Double Met. Cyanide Catal.* **2008**, 434–435.
[106] M. Pohl, E. Danieli, M. Leven, W. Leitner, B. Blümich, T. E. Müller, *Macromolecules* **2016**, *49*, 8995–9003.
[107] C. T. Cohen, G. W. Coates, in *J. Polym. Sci. Part A Polym. Chem.* **2006**, pp. 5182–5191.
[108] J. K. Varghese, A. Cyriac, B. Y. Lee, *Polyhedron* **2012**, *32*, 90–95.
[109] N. Almora-Barrios, S. Pogodin, L. Bellarosa, M. García-Melchor, G. Revilla-López, M. García-Ratés, A. B. Vázquez-García, P. Hernández-Ariznavarreta, N. López, *ChemCatChem* **2015**, *7*, 928–935.
[110] T. G. Fox, P. J. Flory, *J. Appl. Phys.* **1950**, *21*, 581–591.
[111] D.-J. Liaw, P.-S. Chen, *J. Polym. Sci. Part A Polym. Chem.* **1996**, *34*, 885–891.
[112] D. Liaw, W. Shen, *Angew. Makromol. Chem.* **1992**, *199*, 171–190.
[113] L. Luo, Y. Meng, T. Qiu, X. Li, *J. Appl. Polym. Sci.* **2013**, *130*, 1064–1073.
[114] K. Yasuda, R. C. Armstrong, R. E. Cohen, *Rheol. Acta* **1981**, *20*, 163–178.

Manuscript received: April 16, 2019
Revised manuscript received: May 12, 2019